

## Electronic Supplementary Information for

### Application of three-coordinate copper(I) complexes with halide ligands in organic light-emitting diodes that exhibit delayed fluorescence

Masahisa Osawa,\* Mikio Hoshino, Masashi Hashimoto, Isao Kawata, Satoshi Igawa, and  
Masataka Yashima

#### Contents

Experimental Detail	page
1. Crystal Structure determination	S2
<b>Table S1</b> Crystallographic data for <b>5</b>	
2. NMR Experiments	S3–S5
<b>Fig. S1</b> $^1\text{H}$ NMR spectrum of <b>4</b> in $\text{CD}_2\text{Cl}_2$ at 220 K.	
<b>Fig. S2</b> $^{13}\text{C}$ { $^1\text{H}$ } NMR spectrum of <b>4</b> in $\text{CD}_2\text{Cl}_2$ at 220 K.	
<b>Fig. S3</b> $^{31}\text{P}$ { $^1\text{H}$ } NMR spectrum of <b>4</b> in $\text{CD}_2\text{Cl}_2$ at 220 K.	
<b>Fig. S4</b> $^1\text{H}$ NMR spectrum of <b>5</b> in $\text{CD}_2\text{Cl}_2$ at 220 K.	
<b>Fig. S5</b> $^{13}\text{C}$ { $^1\text{H}$ } NMR spectrum of <b>5</b> in $\text{CD}_2\text{Cl}_2$ at 220 K.	
<b>Fig. S6</b> $^{31}\text{P}$ { $^1\text{H}$ } NMR spectrum of <b>5</b> in $\text{CD}_2\text{Cl}_2$ at 220 K.	
3. Temperature dependence of lifetime	S6–S8
<b>Fig. S7</b> Temperature dependence of lifetime for <b>1</b> .	
<b>Fig. S8</b> Temperature dependence of lifetime for <b>3</b> .	
<b>Fig. S9</b> Temperature dependence of lifetime for <b>4</b> .	
<b>Fig. S10</b> Temperature dependence of lifetime for <b>5</b> .	
4. Theoretical Studies	S8–S10
<b>Fig. S11</b> Optimized core structures of <b>1</b> in the ground state ( $S_0$ ), the singlet ( $S_1$ ) and the triplet ( $T_1$ ) excited states.	
<b>Fig. S12</b> Optimized core structures of <b>2</b> in $S_0$ , $S_1$ , and $T_1$ .	
<b>Fig. S13</b> Optimized core structures of <b>3</b> in $S_0$ , $S_1$ , and $T_1$ .	
<b>Fig. S14</b> The sum of the angles around P1 and P2 in each optimized structure of <b>1</b> .	
<b>Fig. S15</b> The sum of the angles around P1 and P2 in each optimized structure of <b>3</b> .	
<b>Fig. S16</b> (A) The molecular structure of <b>3</b> determined using X-ray structural analysis. (B) The optimized $S_0$ structure of <b>3</b> .	
5. Photophysical properties of amorphous films	S11
<b>Table S2</b> Doping concentration dependence of PLQE for <b>2</b> in mCP	
6. Luminance-Current Efficiency Characteristic	
<b>Fig. S17</b> Luminance-Current Efficiency Characteristic	

## Experimental Detail

### 1. Crystal Structure determination

**Table S1** Crystallographic data for **5**

<b>5</b>	
formula	C <sub>42</sub> H <sub>48</sub> BrCuP <sub>2</sub>
formula weight	758.24
cryst syst	Orthorhombic
space group	Pna2 <sub>1</sub>
<i>a</i> / Å	20.5325(19)
<i>b</i> / Å	9.3801(9)
<i>c</i> / Å	19.4895(15)
<i>V</i> / Å <sup>3</sup>	1679.05 (4)
<i>Z</i>	4
<i>d</i> <sub>calcd</sub> / g cm <sup>-3</sup>	1.342
<i>T</i> / K	90(2)
radiation	Mo Kα (λ = 0.71073 Å)
μ / cm <sup>-1</sup>	1.763
diffractometer	Rigaku AFC-8
max 2θ / deg	60
reflns colld	24700
indep reflns	9995 (Rint = 0.0394)
no. of param refined	415
<i>RI</i> , <sup>[a]</sup> <i>wR2</i> ( <i>I</i> > 2σ <i>I</i> ) <sup>[b]</sup>	0.0342, 0.0619
<i>S</i>	0.979

[a] *RI* = Σ||*Fo*| - |*Fc*||/Σ|*Fo*|. [b] *wR2* = [Σ*w*(|*Fo*| - |*Fc*|)<sup>2</sup>/Σ*w*|*Fo*|<sup>2</sup>]<sup>1/2</sup>

## 2. NMR Experiments

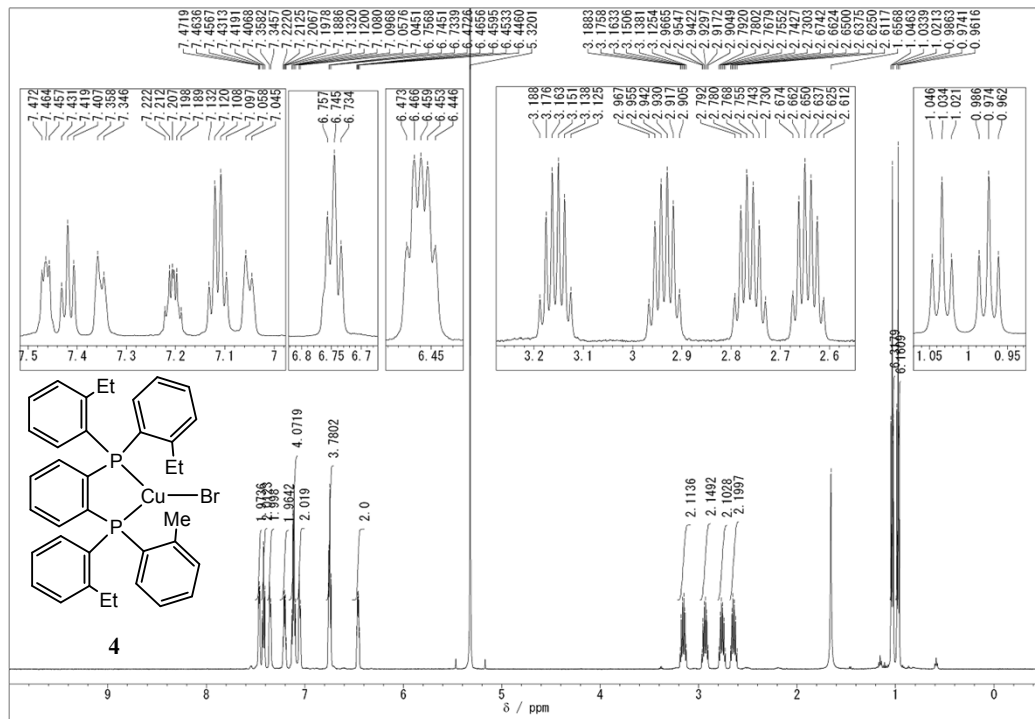


**Figure S1.**  $^1\text{H}$  NMR spectrum of **4** in  $\text{CD}_2\text{Cl}_2$  at 220 K.

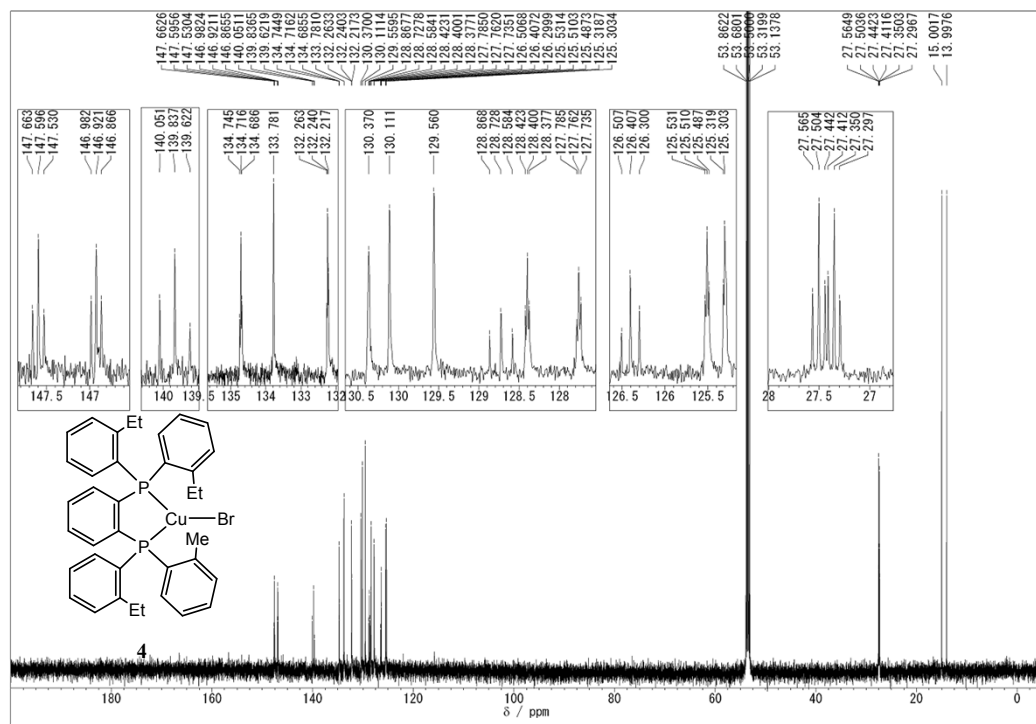


**Figure S2.**  $^{13}\text{C}$  { $^1\text{H}$ } NMR spectrum of **4** in  $\text{CD}_2\text{Cl}_2$  at 220 K.

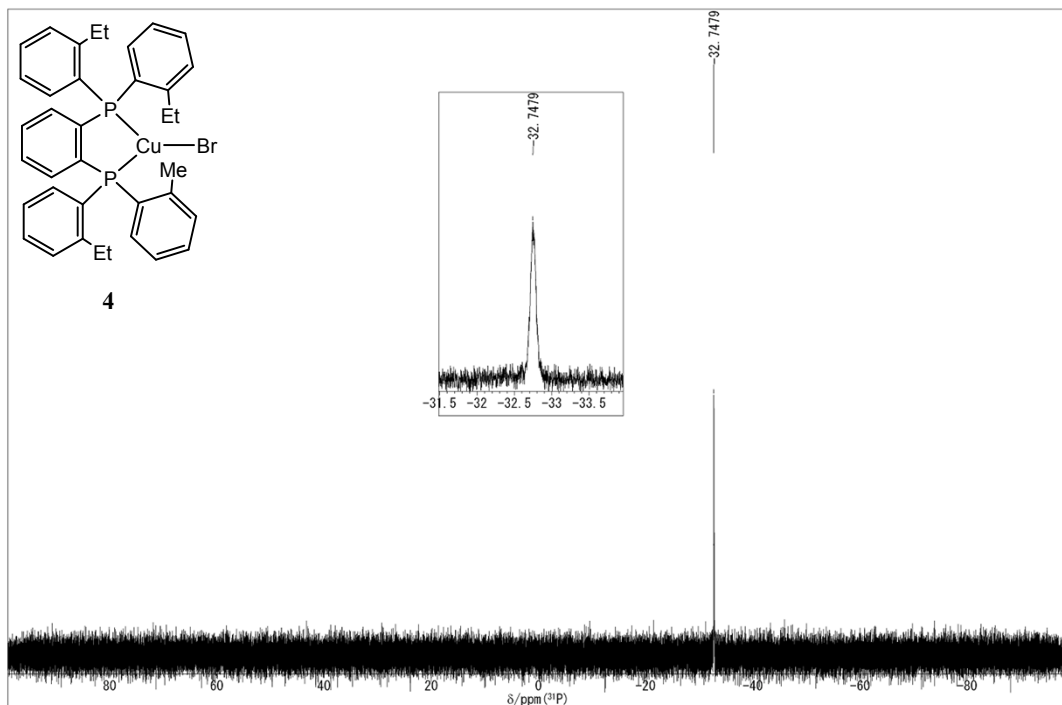


**Figure S3.**  $^{31}\text{P}$   $\{^1\text{H}\}$  NMR spectrum of **4** in  $\text{CD}_2\text{Cl}_2$  at 220 K.

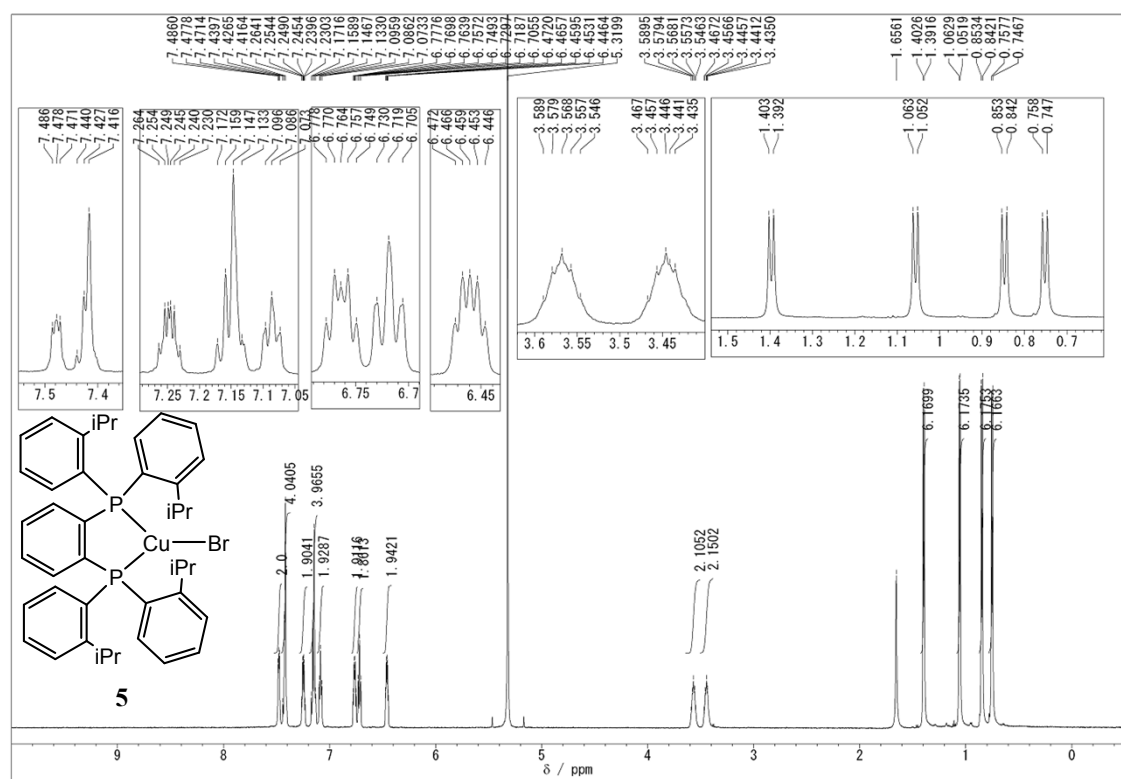


**Figure S4.**  $^1\text{H}$  NMR spectrum of **5** in  $\text{CD}_2\text{Cl}_2$  at 220 K.

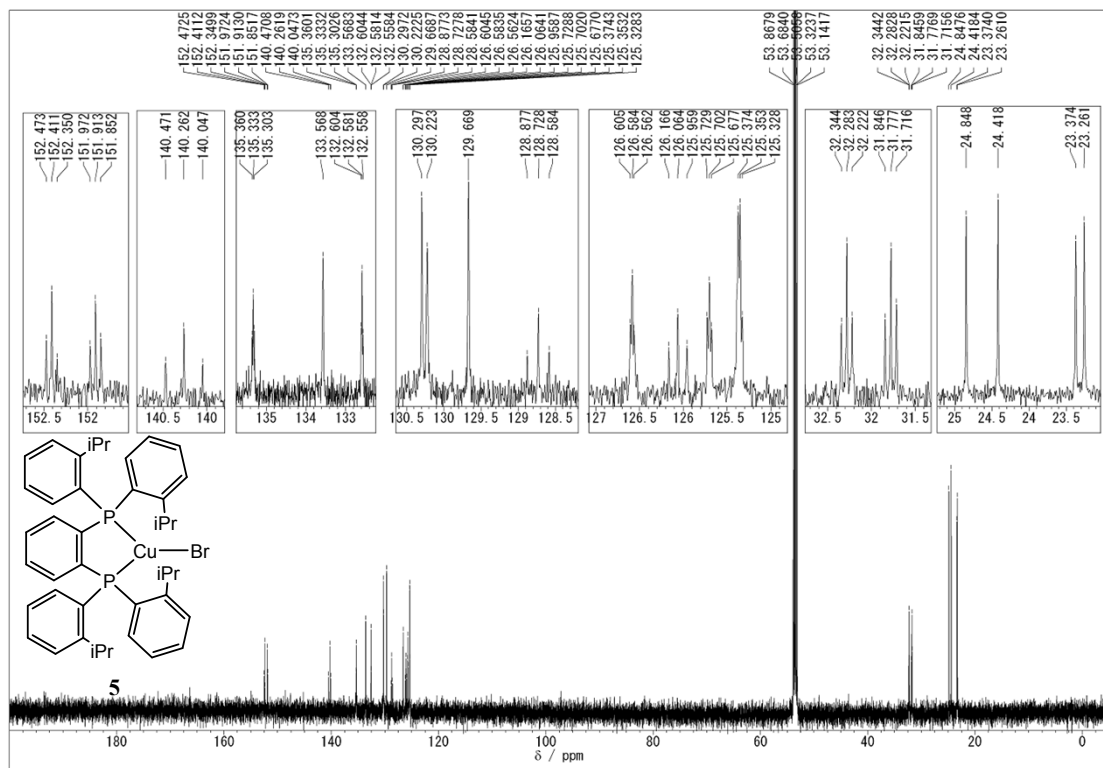


**Figure S5.**  $^{13}\text{C}$  { $^1\text{H}$ } NMR spectrum of **5** in  $\text{CD}_2\text{Cl}_2$  at 220 K.

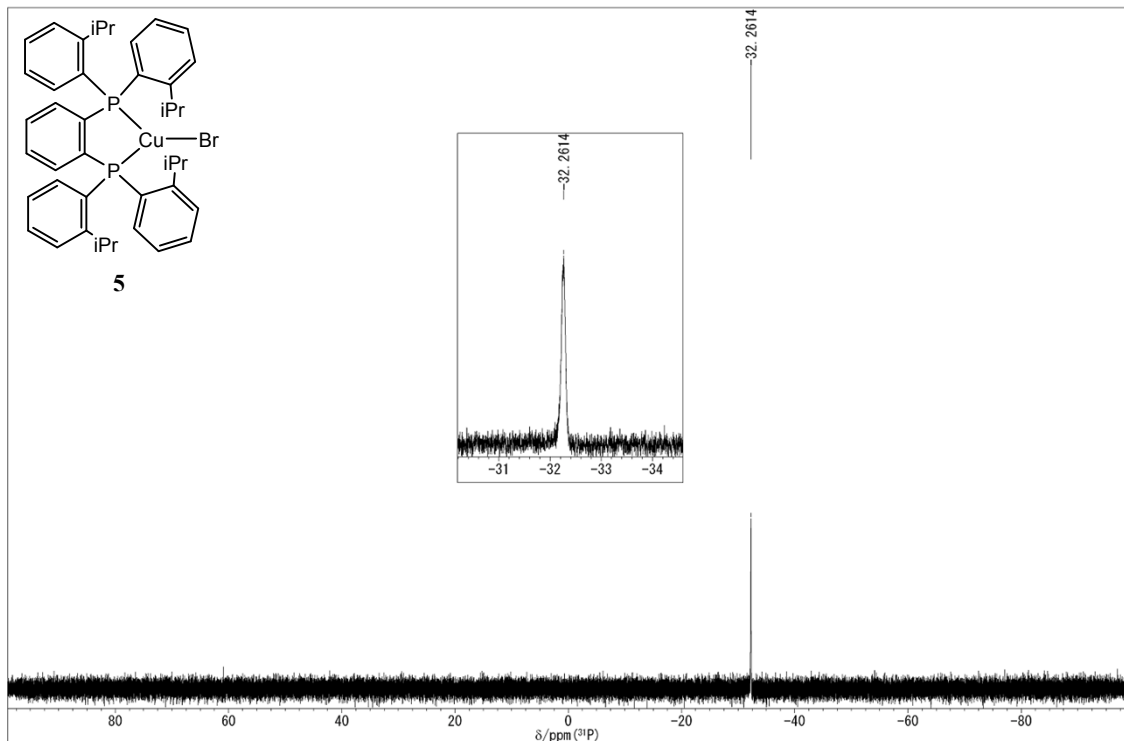


**Figure S6.**  $^{31}\text{P}$  { $^1\text{H}$ } NMR spectrum of **5** in  $\text{CD}_2\text{Cl}_2$  at 220 K.

### 3. Temperature dependence of lifetime

[Fitting procedure A for **1** and **4**]

$\tau_T$  (decay time from of the  $T_1$  state),  $\tau_S$  (decay time of the prompt fluorescence), and  $\Delta E(S_1 - T_1)$  (activation energy) were determined from a fit of Eq. 1 to measured  $\tau_{av}$  (25 points) by least-square method.

[Fitting procedure B for **2**, **3**, and **5**]

$\tau_S$  (decay time of the prompt fluorescence) and  $\Delta E(S_1 - T_1)$  (activation energy) were determined from a fit of Eq. 1 to measured  $\tau_{av}$  (25 points) by least-square method.

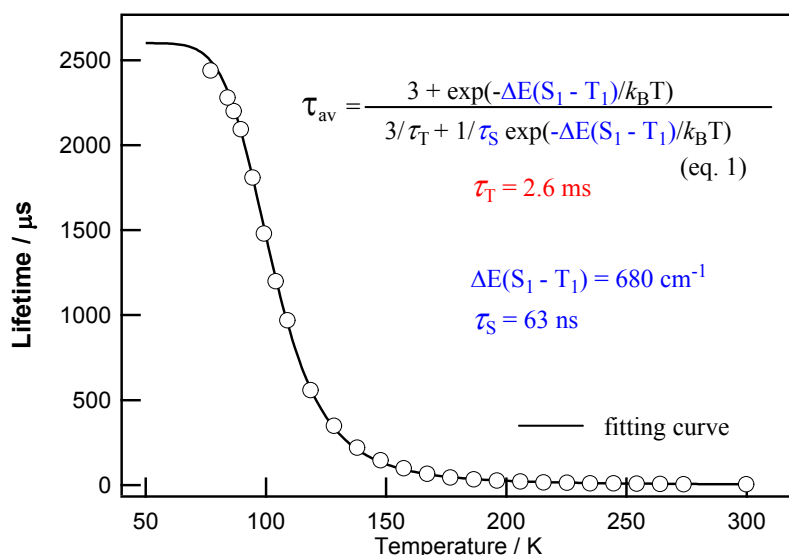


**Fig. S7** Temperature dependence of lifetime for **1**.

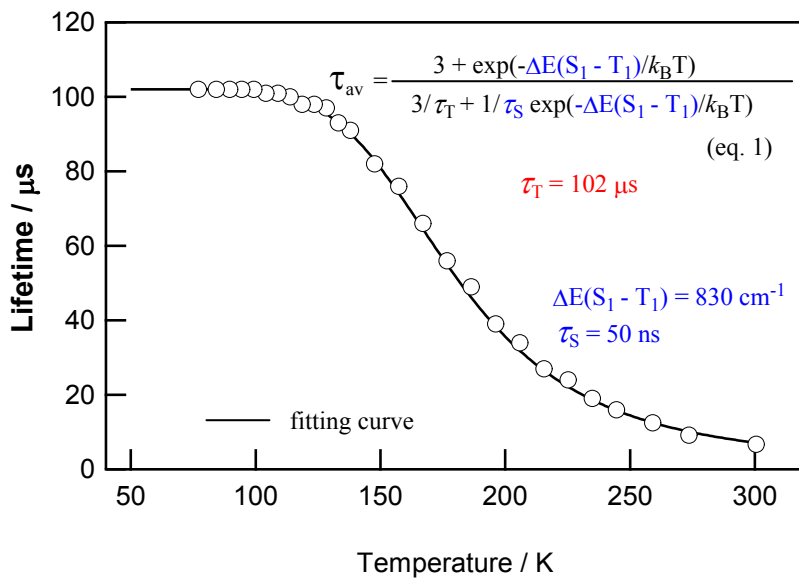


**Fig. S8** Temperature dependence of lifetime for **3**. The  $t_T = 102 \mu\text{s}$  measured at 77 K was used for the curve fitting by eq. 1.

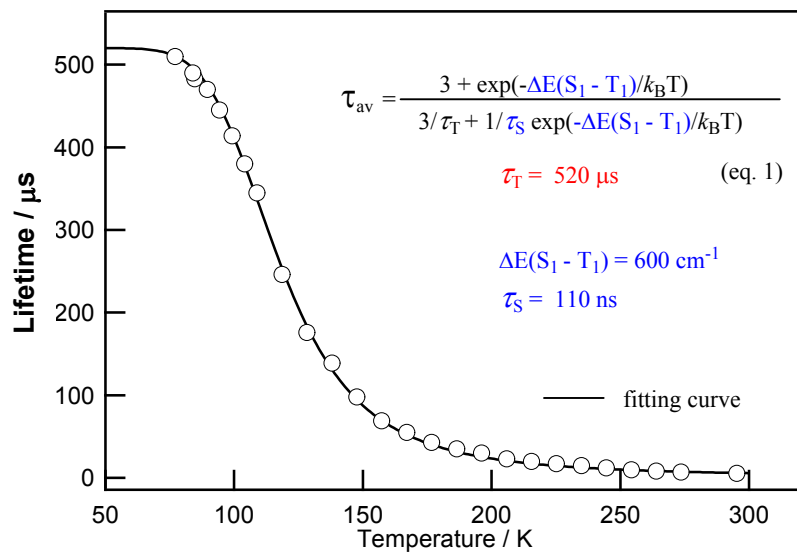


**Fig. S9** Temperature dependence of lifetime for **4**.

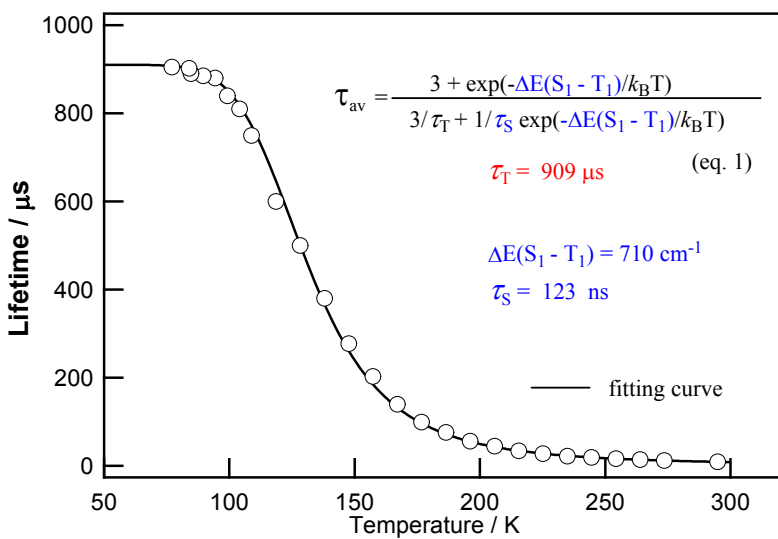


**Fig. S10** Temperature dependence of lifetime for **5**. The  $t_T = 909 \mu\text{s}$  measured at 77 K was used for the curve fitting by eq. 1.

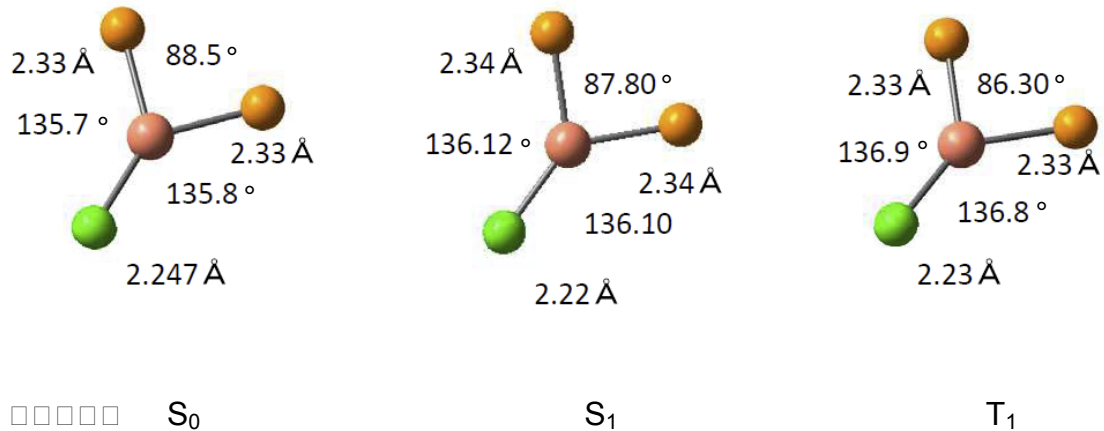


**Fig. S11** Optimized core structures of **1** in the ground state ( $S_0$ ), the singlet ( $S_1$ ) and the triplet ( $T_1$ ) excited states.

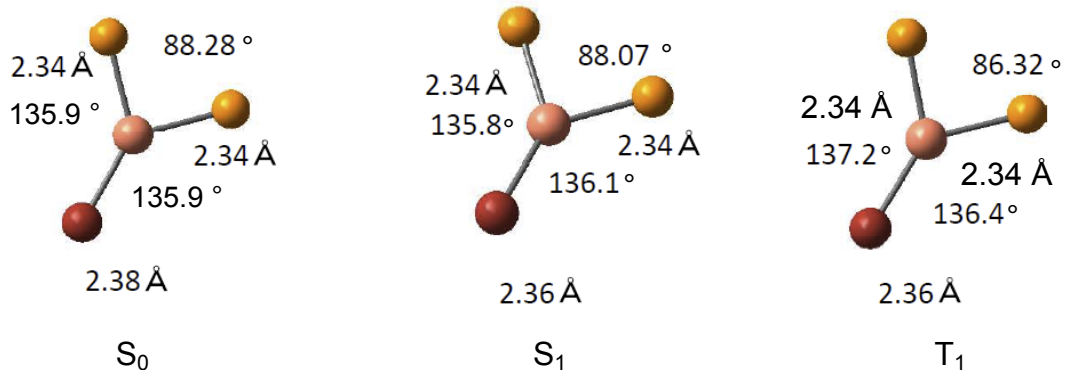


**Fig. S12** Optimized core structures of **2** in  $S_0$ ,  $S_1$ , and  $T_1$ .

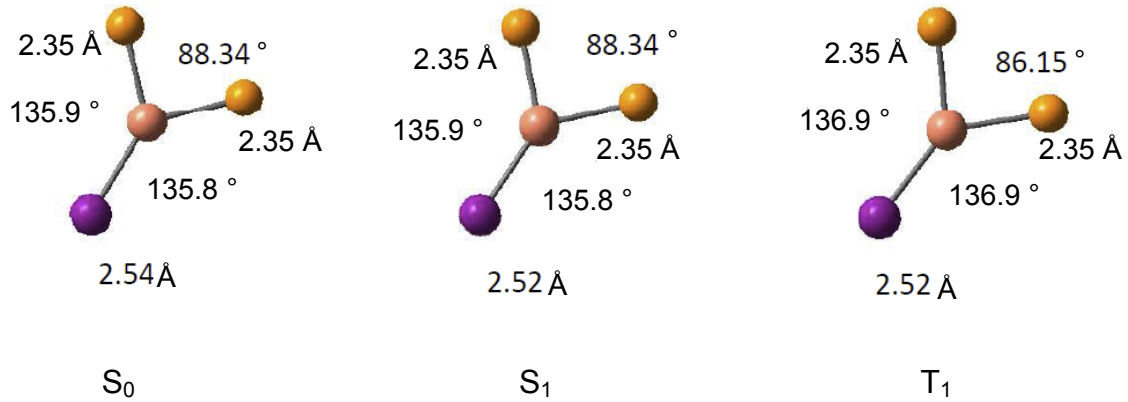


**Fig. S13** Optimized core structures of **3** in  $S_0$ ,  $S_1$ , and  $T_1$ .

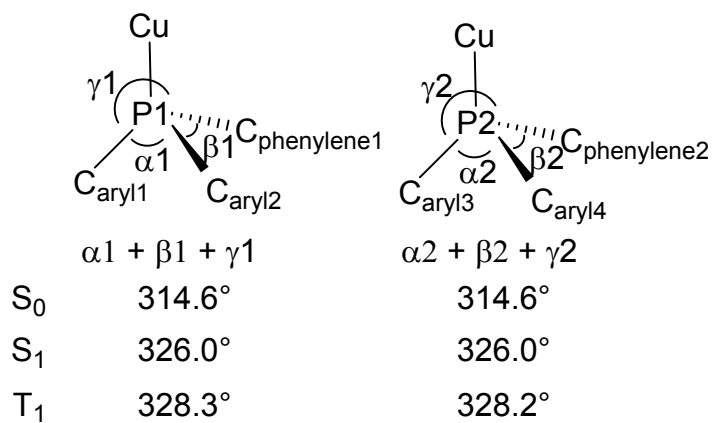


**Fig. S14** The sum of the angles around P1 and P2 in each optimized structure of **1**.

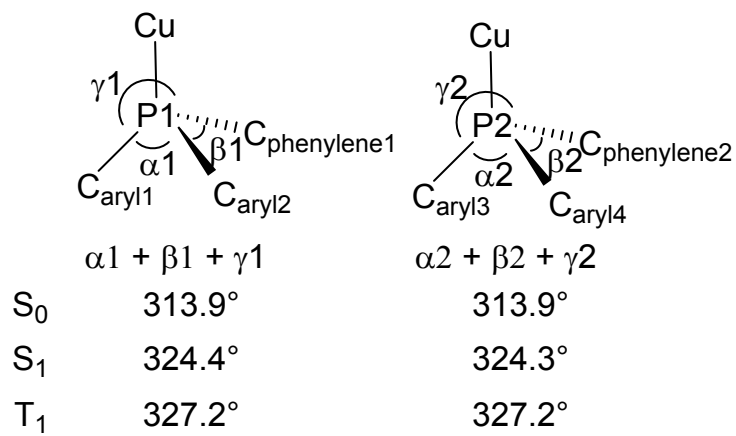


**Fig. S15** The sum of the angles around P1 and P2 in each optimized structure of **3**.

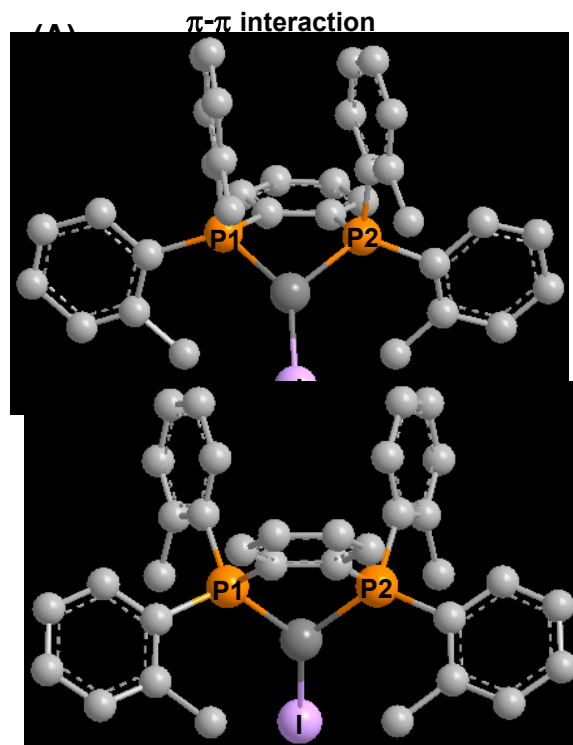


**Fig. S16** (A) The molecular structure of **3** determined using X-ray structural analysis. (B) The optimized  $S_0$  structure of **3**.

Doping concentration (wt%)	5%	10%	20%	100%
PLQE / %	65	71	61	38

**Table S2** Doping concentration dependence of PLQE for **2** in mCP;  $\lambda_{\text{exc}} = 355$  nm.

## 6. Luminance-Current Efficiency Characteristic

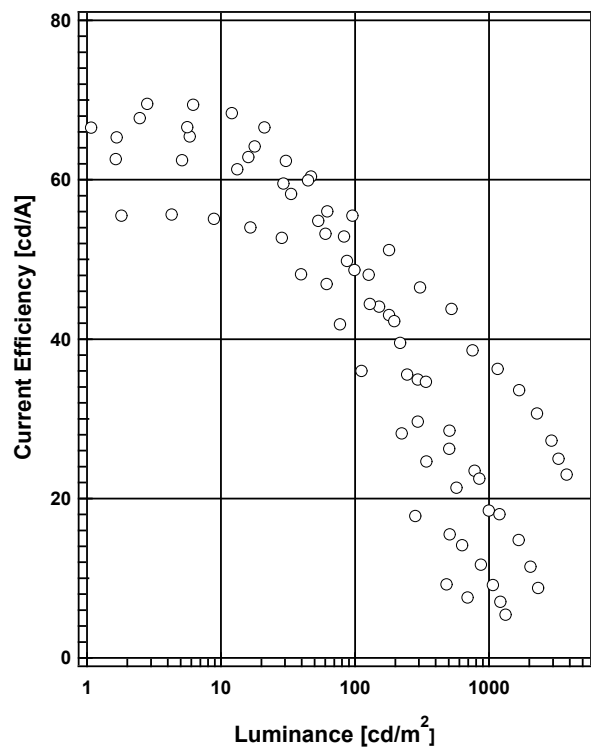


**Fig. S17** Luminance-Current Efficiency Characteristic